Achieving high sensing sensitivity in Dy^{3+} doped garnet phosphor toward optical thermometry

Shichang Long [a,b], Minfeng Tian [a], Dan Zhang [b], Xixian Luo [b], Wen Xu [b], Ying Tian [a*], Shuangyu Xin [b*]

[a] Department of applied physics, Dalian Maritime University, Dalian 116026, China.
[b] School of Physics and Materials Engineering, Dalian Minzu University, Dalian, Liaoning, 116600, China

* E-mail address: tianying@dlmu.edu.cn (Ying Tian); xinshuangyu@dlnu.edu.cn (Shuangyu Xin)

Experimental section

Materials and Synthesis

A series of $Ca_{2.5-x}Hf_{2.5}Ga_3O_{12}$: $x$$Dy^{3+}$ phosphors were synthesized by solid-state reaction at high temperature. The primary reagent used in this experiment were $CaCO_3$ (Macklin, 99.5%), HfO_2 (Macklin, 99.9%), Ga_2O_3 (Macklin, 99.99%) and Dy_2O_3 (Macklin, 99.9%), each of these components was assigned a weight proportional to their stoichiometric ratio. The weighed reagent were completely mixed and grounded thoroughly for 30 minutes in an agate mortar, and the final mixtures were heated up to 1400°C for 6 hours. Finally, the phosphors were successfully prepared after cooling to room temperature.

Characterization

The powder X-ray diffraction (XRD) analysis was deployed to evaluate the phase purity and crystal structure using Cu Kα radiation (λ = 1.54056 Å) with settings of 40 kV and 30 mA. The morphology of sintered CHGO: Dy^{3+} phosphors were characterized by JEM-2100F transmission electron microscopy (TEM). The photoluminescence excitation (PLE) and PL spectra, temperature emission spectra, and decay curves of the phosphors were measured by Edinburgh FLS-1000 fluorescence spectrophotometer equipped with an accessory for temperature-control and microsecond light source. In addition, the elemental composition was analyzed using energy dispersive X-ray spectroscope (EDS). The diffuse reflectance spectra (DRS) were obtained by a Lambda

750 UV-Vis-NIR spectrophotometer. The electroluminescence (EL) spectra were measured using optical fiber spectrometer (HR-6XR300-10) measuring system under a drive current of 100-600 mA. The temperature variations of the phosphor-converted light-emitting diode (pc-LED) were captured using a FLUKE Ti32 thermal imaging camera as the driving currents were incrementally increased from 100 to 600 mA.

Table S1 Optical thermometric parameters in Er^{3+} doped materials

Materials	λ_{ex} (nm)	S_r (% K^{-1})	S_a (% K^{-1})	Ref
$BiPO_4$: Er^{3+}/Yb^{3+}	980	0.0111@313 K	1.22@548 K	1
$Ba_2TiGe_2O_8$: Er^{3+}/Yb^{3+}	980	0.0107@333 K	0.59@573 K	2
$LaBMoO_6$: Er^{3+}/Yb^{3+}	980	1.1600@300 K	/	3
Gd_2O_3: Er^{3+}/Yb^{3+}	980	1.7200@301 K	1.27@574 K	4
$NaGdF_4$: Er^{3+}/Yb^{3+}	980	0.0119@303 K	0.40@563 K	5
$BaMgF_4$: Er^{3+}/Yb^{3+}	980	0.0131@323 K	0.83@583 K	6
LaF_3: Er^{3+}/Yb^{3+}	980	1.3000@150 K	3.50@400 K	7
$Sc_2(MoO_4)_3$: Er^{3+}/Yb^{3+}	980	12.3000@298 K	/	8
Sc_2O_3: Er^{3+}/Yb^{3+}	980	0.5340@364 K	0.13@290 K	9
$Ba_5Gd_8Zn_4O_{21}$: Er^{3+}/Yb^{3+}	980	0.0169@260 K	0.32@490 K	10

Table S2 Crystallographic data of CHGO and CHGO: 0.01Dy^{3+}

Formula	CHGO	CHGO: 0.01Dy^{3+}
Space group	Ia-3d (230)	Ia-3d (230)
Crystal system	Cubic	Cubic
α = β = γ (°)	90	90
a = b= c(Å)	12.56653	12.53005
V (Å^3)	1984.477	1983.121
R_p (%)	9.79	11.15
R_{wp} (%)	7.12	9.18
χ^2	1.14	1.49

Table S3 The crystallographic atomic positions of CHGO: 0.01Dy^{3+} based on the refinement

Atom	x	y	z	occup.	uiso	Site
O	0.09160	0.19228	0.27493	1.000	0.014	96h
Ga	0.37500	0.00000	0.25000	1.000	-0.027	24d
Ca	0.12500	0.00000	0.25000	0.825	-0.025	24c
Hf1	0.12500	0.00000	0.25000	0.167	-0.025	24c
Hf2	0.00000	0.00000	0.00000	1.000	-0.032	16a
Dy	0.12500	0.00000	0.25000	0.008	-0.025	24c

Table S4 Maximum S_a and S_r in CHGO: 0.01Dy^{3+} phosphors.

Intensity ratio scheme	Temperature	S_a ($\%K^{-1}$)	S_r ($\%K^{-1}$)
I_{457}/I_{483}	298-523K	0.10@523 K	2.08@298 K
I_{457}/I_{495}	298-523K	0.13@523 K	2.12@298 K
I_{457}/I_{582}	298-523K	0.09@523 K	2.07@298 K
I_{457}/I_{675}	298-523K	2.51@523 K	1.55@298 K

Table S5. Comparison of Dy^{3+} doped materials as luminescent ratiometric thermometers.

Host: Dy^{3+}	Temperature range	$S_{r\text{-}max}$($\%K^{-1}$)	$S_{a\text{-}max}$($\%K^{-1}$)	Ref.
$Li_3Y_3Te_2O_{12}$: Dy^{3+}	80-300 K	1.20@80 K	2.000@80 K	11
$GdVO_4$: Dy^{3+}	300-473 K	2.00@300 K	0.399@473 K	12
LaF_3: Dy^{3+}	298-523 K	2.02@298 K	0.020@523 K	13
YVO_4: Dy^{3+}	298-673 K	1.66 @298 K	0.033@673 K	14
$Sr_2NaMg_2V_3O_{12}$: Dy^{3+}	250-500 K	1.90 @380 K	/	15
$LiNbO_3$: Dy^{3+}	295-775 K	1.89 @298 K	0.060@700 K	16
CHGO: Dy^{3+}	298-523 K	2.12@298 K	2.510@523 K	This work

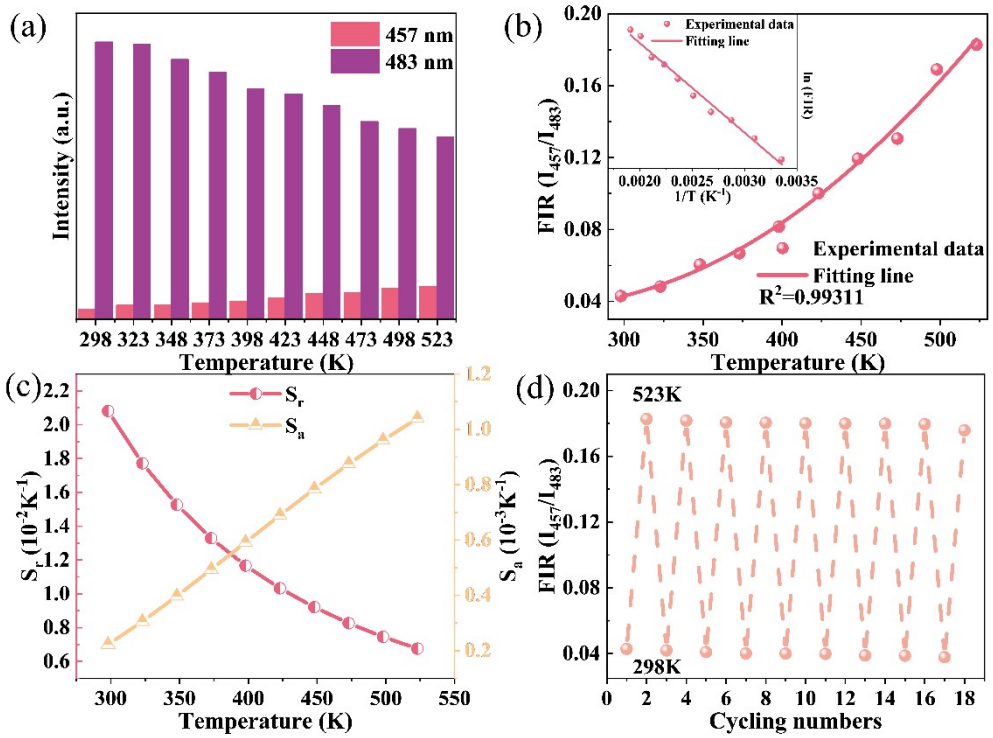

Figure S1a) The integrated fluorescence intensities of the PL peaks at 457 and 483 nm at different temperatures; b) The fitting curve of FIR (I_{457}/I_{483}) values at various temperatures. The inset shows the correspondence plot of ln (FIR) versus 1/T.; c) The fitting curves of the absolute sensitivity (S_a) and relative sensitivity (S_r) values at different temperatures; d) The repeatability of FIR of CHGO: 0.01Dy^{3+}.

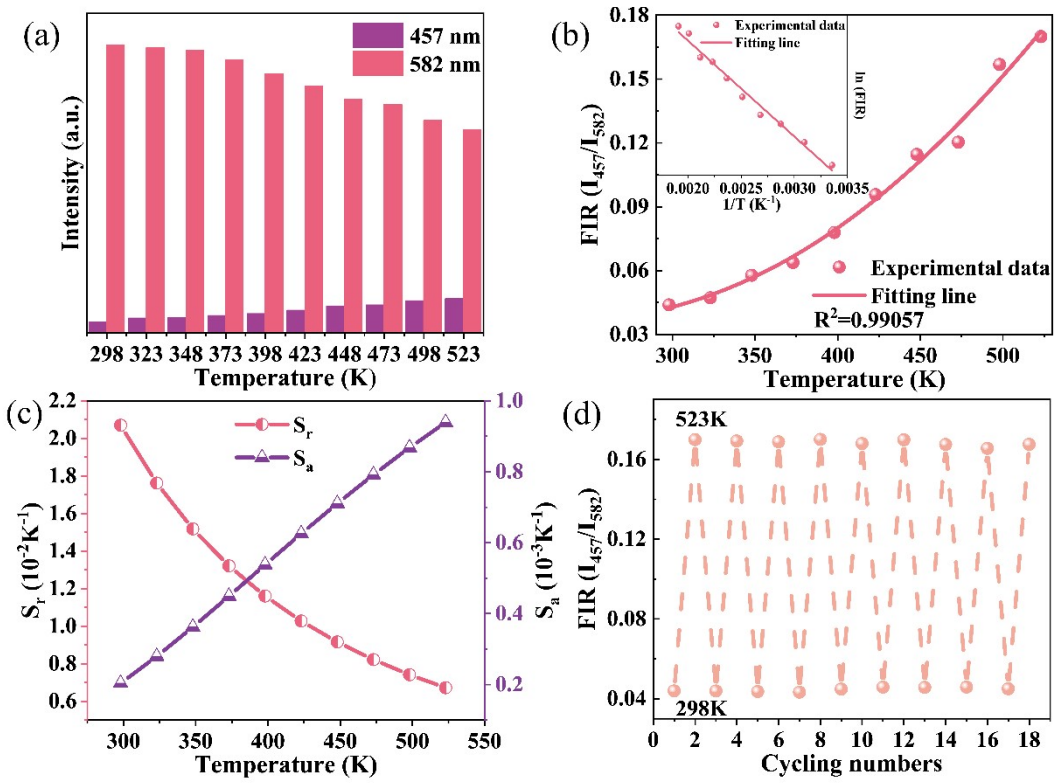

Figure S2a) The integrated fluorescence intensities of the PL peaks at 457 and 582 nm at different temperatures; b) The fitting curve of FIR (I_{457}/I_{582}) values at various temperatures. The inset shows the correspondence plot of ln (FIR) versus 1/T.; c) The fitting curves of the absolute sensitivity (S_a) and relative sensitivity (S_r) values at different temperatures; d) The repeatability of FIR of CHGO: $0.01Dy^{3+}$.

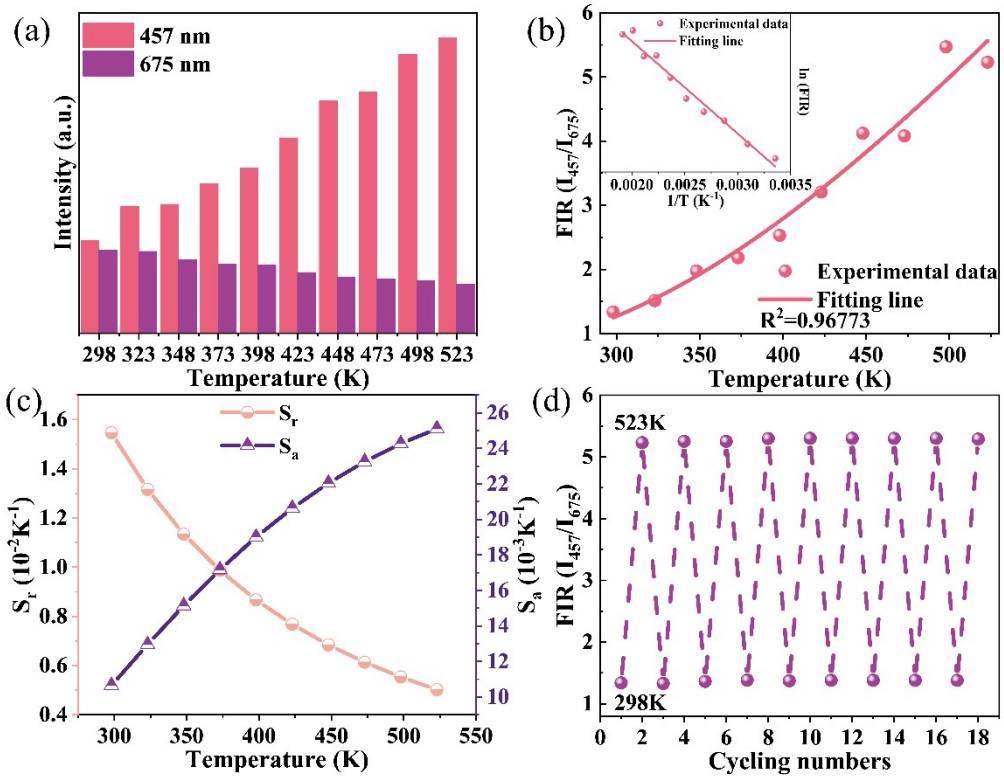

Figure S3a) The integrated fluorescence intensities of the PL peaks at 457 and 675 nm at different temperatures; b) The fitting curve of FIR (I_{457}/I_{675}) values at various temperatures. The inset shows the correspondence plot of ln (FIR) versus 1/T.; c) The fitting curves of the absolute sensitivity (S_a) and relative sensitivity (S_r) values at different temperatures; d) The repeatability of FIR of CHGO: 0.01Dy^{3+}.

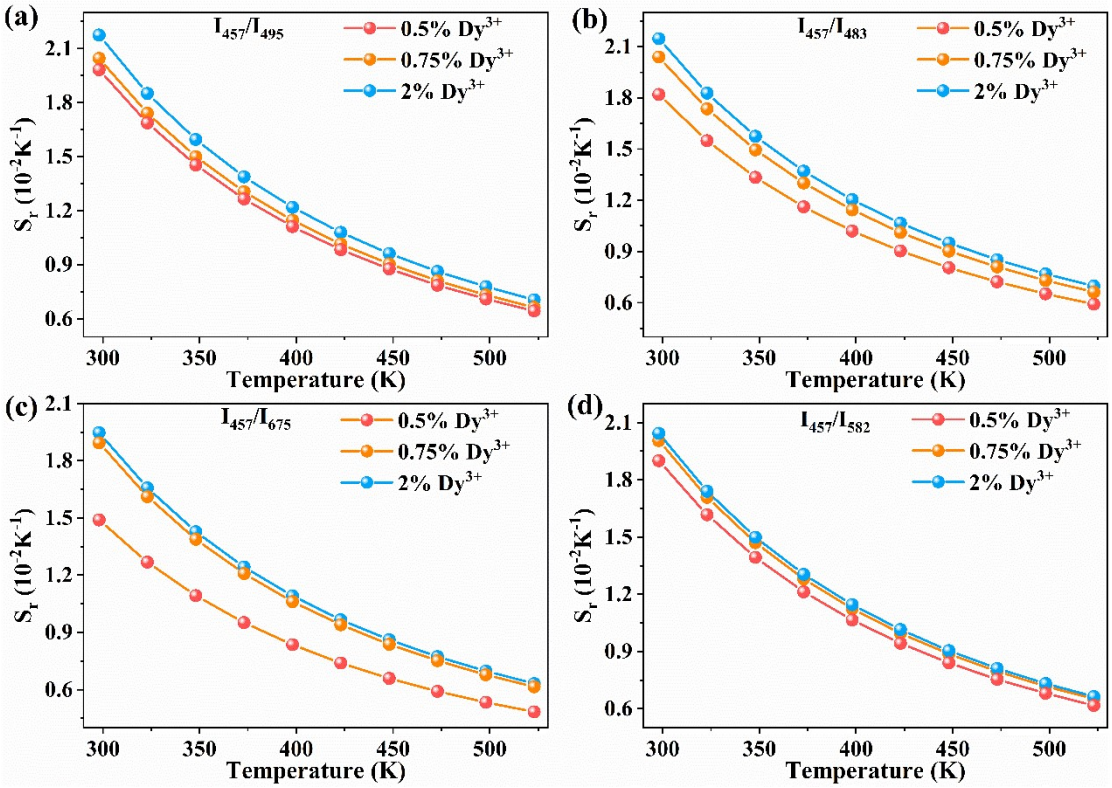

Figure S4 The S_r values of the CHGO: xDy^{3+}(x = 0.5%, 0.75% and 2%) phosphors for I_{457}/I_{495} (a), I_{457}/I_{483} (b), I_{457}/I_{675} (c) and I_{457}/I_{582} (d).

References

1. N. Wang, Z. Fu, Y. Wei and T. Sheng, Investigation for the upconversion luminescence and temperature sensing mechanism based on $BiPO_4$: Yb^{3+}, RE^{3+} (RE^{3+}= Ho^{3+}, Er^{3+} and Tm^{3+}), *J. Alloys. Compd.,* 2019, **772**, 371-380.
2. B. Hou, M. Jia, P. Li, G. Liu, Z. Sun and Z. Fu, Multifunctional optical thermometry based on the rare-earth-ions-doped up-/down-conversion $Ba_2TiGe_2O_8$: Ln (Ln = Eu^{3+}/Er^{3+}/Ho^{3+}/Yb^{3+}) phosphors, *Inorg. Chem,* 2019, **58**, 7939-7946.
3. X. Li, B. Bao, X. He, G. Wang, Y. Huang, L. Li and Y. Yu, Optical temperature sensing with an Er^{3+}, Yb^{3+} co-doped $LaBMoO_6$ single crysta, *J. Mater. Chem. C,* 2023, **11**, 2494-2504.
4. Z. Li, Q. Han, T. Yan, Z. Huang, Y. Song, Y. Wang and X. Zhang, Up-conversion luminescence and optical temperature sensing of Er^{3+}, Yb^{3+} co-doped Gd_2O_3 phosphors with different F-/Ln^{3+}, *J. Alloys. Compd,* 2022, **904**, 164009.

5. D. Chen, S. Liu, X. Li, Z. Wan and S. Li, Gd-based oxyfluoride glass ceramics: phase transformation, optical spectroscopy and upconverting temperature sensing, *J. Eur. Ceram. Soc,* 2017, **37**, 4083-4094.
6. B. P. Kore, A. Kumar, L. Erasmus, R. E. Kroon, J. J. Terblans, S. J. Dhoble and H. C. Swart, Energy transfer mechanisms and optical thermometry of $BaMgF_4$: Yb^{3+}, Er^{3+} phosphor, *Inorg. Chem,* 2018, **57**, 288-299.
7. H. Zhang, X. Dong, L. Jiang, Y. Yang, X. Cheng and H. Zhao, Comparative analysis of upconversion emission of LaF_3: Er/Yb and LaOF: Er/Yb for temperature sensing, *J. Mol. Struct.,* 2020, **1206**, 127665.
8. J. Liao, M. Wang, F. Lin, Z. Han, B. Fu, D. Tu, X. Chen, B. Qiu and H.-R. Wen, Thermally boosted upconversion and downshifting luminescence in $Sc_2(MoO_4)_3$: Yb/Er with two-dimensional negative thermal expansion, *Nat. Commun,* 2022, **13**, 2090.
9. H. L. Zhou, K. S. Zhu, J. Wang, L. H. Ye, J. X. Zhang and L. G. Wang, Effects of $Er^{3+}$and Yb^{3+}concentrations on upconversion luminescence and thermal sensing characteristics of Sc_2O_3: Er^{3+}/Yb^{3+}phosphors, *Ceram. Int,* 2024, **50**, 1947-1955.
10. H. Suo, C. Guo and T. Li, Broad-scope thermometry based on dual-color modulation up-conversion phosphor $Ba_5Gd_8Zn_4O_{21}$: Er^{3+}/Yb^{3+}, *J. Phys. Chem. C,* 2016, **120**, 2914-2924.
11. A. Bindhu, J. I. Naseemabeevi and S. Ganesanpotti, Insights into the crystal structure and photophysical response of Dy^{3+} doped $Li_3Y_3Te_2O_{12}$ for ratiometric temperature sensing, *J. Sci. Adv. Mater. Dev,* 2022, **7**, 100444.
12. Z. Antic, M. D. Dramicanin, K. Prashanthi, D. Jovanovic, S. Kuzman and T. Thundat, Pulsed laser deposited dysprosium-doped gadolinium-vanadate thin films for noncontact, self-referencing luminescence thermometry, *Adv. Mater,* 2016, **28**, 7745-7752.
13. Y. Y. Bu, S. J. Cheng, X. F. Wang and X. H. Yan, Optical thermometry based on luminescence behavior of Dy^{3+}-doped transparent LaF_3 glass ceramics *Appl. Phys. A,* 2015, **121**, 1433-1434.
14. I. Kolesnikov, A. Kalinichev, M. Kurochkin, E. Y. Kolesnikov and E. Lähderanta, Structural, luminescence and thermometric properties of nanocrystalline YVO_4: Dy^{3+} temperature and concentration series, *Sci Rep,* 2019, **9**, 2043.

15. A. Bindhu, J. I. Naseemabeevi and S. Ganesanpotti, Augmenting cyan emission in vanadate garnets via Dy^{3+}activation for light emitting devices and multi-mode optical thermometry, *Dalton Trans.,* 2023, **52**, 11705-11715.
16. R. Lisiecki, B. Macalik, R. Kowalski, J. Komar and W. Ryba-Romanowski, Effect of temperature on luminescence of $LiNbO_3$ crystals single-doped with Sm^{3+}, Tb^{3+}, or Dy^{3+} Ions, *Crystals,* 2020, **10**, 1034.